Module holding setup for X-ray tests under steady temperature

An experimental semester project by

Mario Seeli

August 22, 2013

Abstract

This document describes the experimental semester project performed in spring semester 2013 as a part of the physics studies at ETH Zurich. The semester project was about to design a setup for X-ray tests of tracker modules of the Compact Muon Solenoid (CMS) Detector of the Large Hadron Collider (LHC).

In order to understand the circumstances of this semester project, a short introduction of the LHC and CMS are given. Furthermore an X-ray calibration of two different chips are performed and discussed in order to motivate the need of this module holding setup, which is explained in detail.

In the appendices at the end of this document, the engineering drawings made during this project are appended.

Contents

1 Introduction

1.1 Stage I / Stage II division

Because the design of the module holding setup was too much work for a normal semester project, we decided to divide the project into two stages. Stage I contains all parts which are used to perform X-ray calibration tests of 4 modules at the same time at steady temperature down to 10°C.

With Stage II of the module holding setup it will be possible to take measurements at lower temperatures than the normal dew point at room temperature. Stage II will be designed to reach temperatures down to -30°C. For this purpose also Stage I had to be designed in a way to achieve the complicated task of cooling down the setup without condensation. A motivation to calibrate the modules at lower temperature is given in section 3.4.

1.2 Tasks of the semester project

The main task of the semester project was to design the module holding setup. During the manufacturing of the parts, the task was to learn how to calibrate pixel modules with the X-ray tube. At the end of the semester project, the parts of Stage I had to be assembled. Unfortunately there was no time left to make test with the module holding setup.

2 LHC and the CMS Pixel Detector

2.1 The Large Hadron Collider

The LHC is the world's most powerful and largest synchrotron, located at CERN, Geneva. It lies about 100 m under ground and consists of two beam pipes in which protons travel nearly at the speed of light. Inside the two beam pipes, the particles travel in opposite direction through the tunnel that is 27 kilometer in circumference. There are four crossing points in the LHC, where the particles of the two different beam pipes can collide. Each point is surrounded by a particle detector which detects the new particles created. Each Detector belongs to different Experiments made with the LHC. These are called ALICE, ATLAS, CMS and LHCb.
This semester project is refered to the CMS experiment.

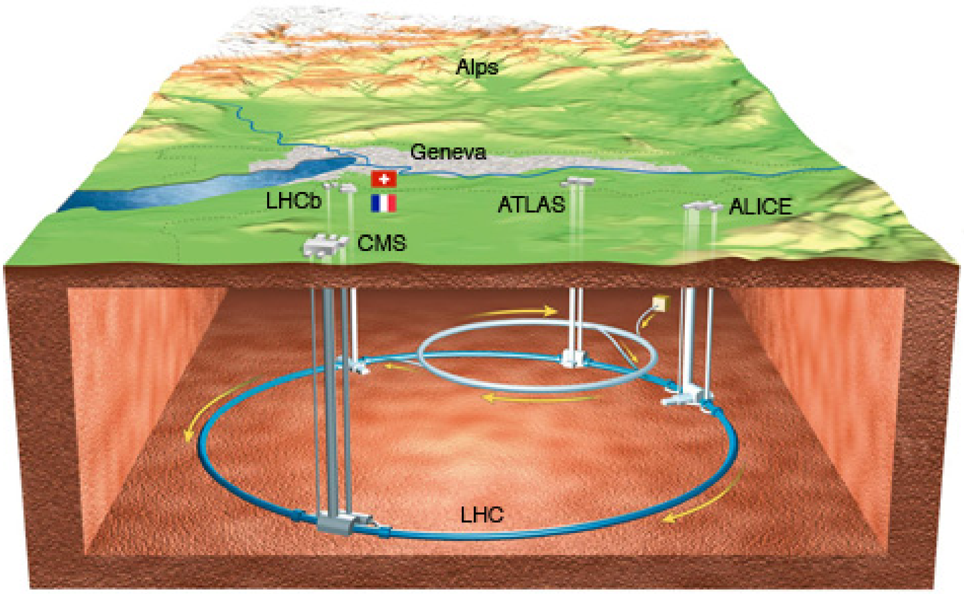

Figure 1: The gigantic Large Hadron Collider which lies about 100 m under ground. Ref: [2]

2.2 General composition of CMS

The CMS detector is built around a huge solenoid magnet, which consists of superconducting wires creating a magnetic field of 4 tesla.
As shown in figure 2 the CMS detector constists of different layers, each fulfills a special task in identifying the different particles: The innermost component is the tracker that is entirely made of silicon. It charts the path of charged particles to determine their momentum as well as the sign of charge. After the Tracker, the particles reach the electromagnetic caloriemeter or ECAL, where electrons and photons produce electromagnetic showers to determine their energy. Hadrons, which do not produce showers in the ECAL, reach the hadron calorimeter or HCAL to determine their energy. These three components are surrounded by the superconducting solenoid. Outside of it, the magnetic field points in the opposite direction. Until here all particles have been stopped except for myons and neutrinos. By which the latter can not be detected by CMS at all. Myons by contrast, which are charged particles can be detected in the myon chambers, which lies outside of the superconducting solenoid. Each kind of particle

can be distinguished by its specific ”signature” in the detector. The track of neutrinos can indirectly be determined by the ”Missing Energy” and the ”Missing Momentum” calculated in the analysis of the whole collision.

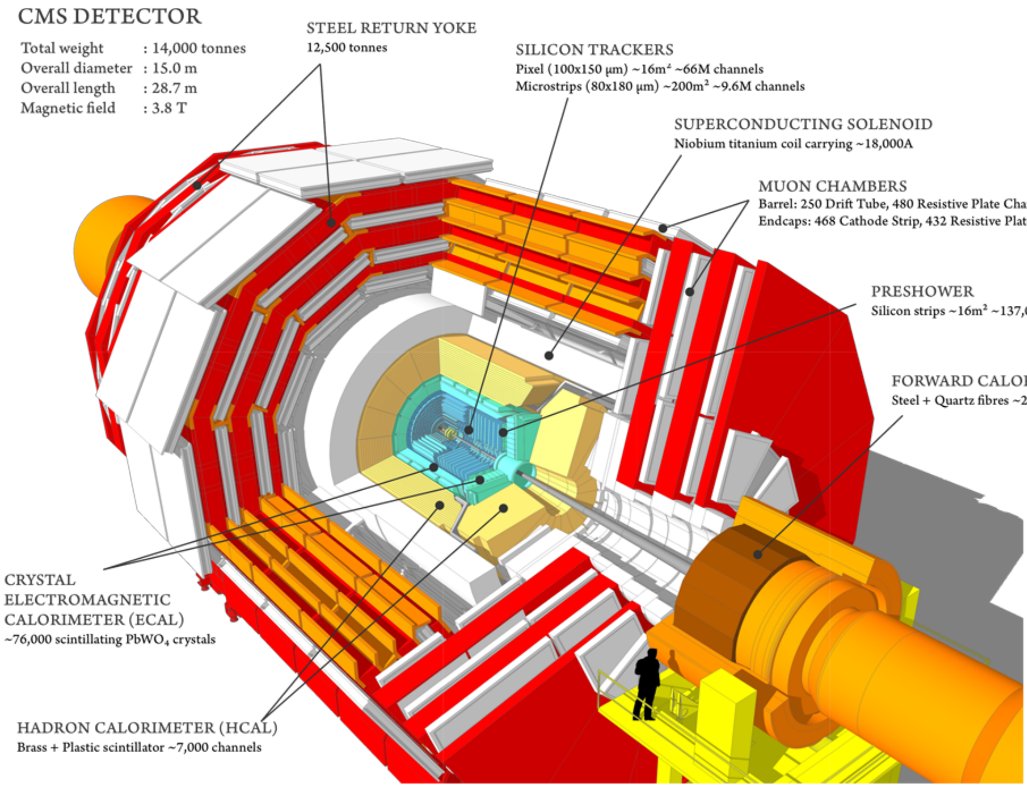

Figure 2: Sectional view of the CMS Detector. Ref: [3]

2.3 CMS Pixel Detector

The CMS Pixel Detector describes the innermost part of the tracking unit of the CMS Detector as shown in figure 3. It ”contains 65 million pixels, allowing it to track the paths of particles emerging from the collision with extreme accuracy. It is also the closest detector to the beam pipe, with cylindrical layers at 4cm, 7cm and 11cm and disks at either end, and so will be vital in reconstructing the tracks of very short-lived particles.” [4] On each layer of the Pixel Detector are Pixel Modules mounted which are composed of 16 quadratic silicon chips each containing 4160 pixels.

2.3.1 Pixel Modules

As mentioned in the previous section, the Pixel Modules consists of 16 silicon chips, each containing 4160 pixels. Such a single chip as well as a Pixel Module are shown in figure 4.
The chips consists of a silicon sensor layer and a readout chip (ROC). A charged particle crossing through a pixel of the silicon sensor generates electron-hole pairs. A bias voltage forces the electrons through a metal bond onto the ROC, which amplifies and analyses the current peak and sends the data out of the detector. A cross-sectional drawing of a pixel as well as the schematic design of a pixel chip is shown in figure 5.

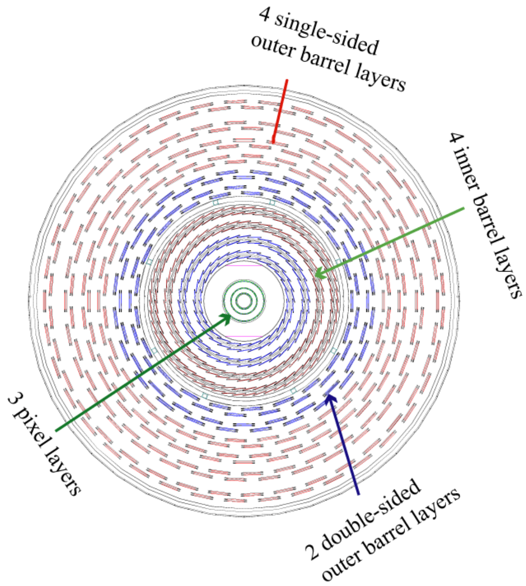

Figure 3: Structure of the CMS tracker unit with the Pixel Detector as the innermost tracking layers. Ref: [3]

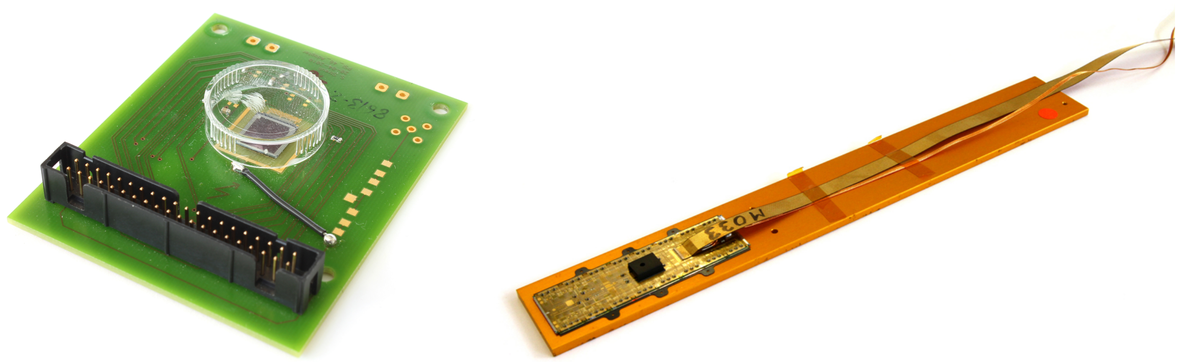

Figure 4: Left: Single silicon chip. [1] Right: Fully assembled CMS pixel module on aluminum handle.

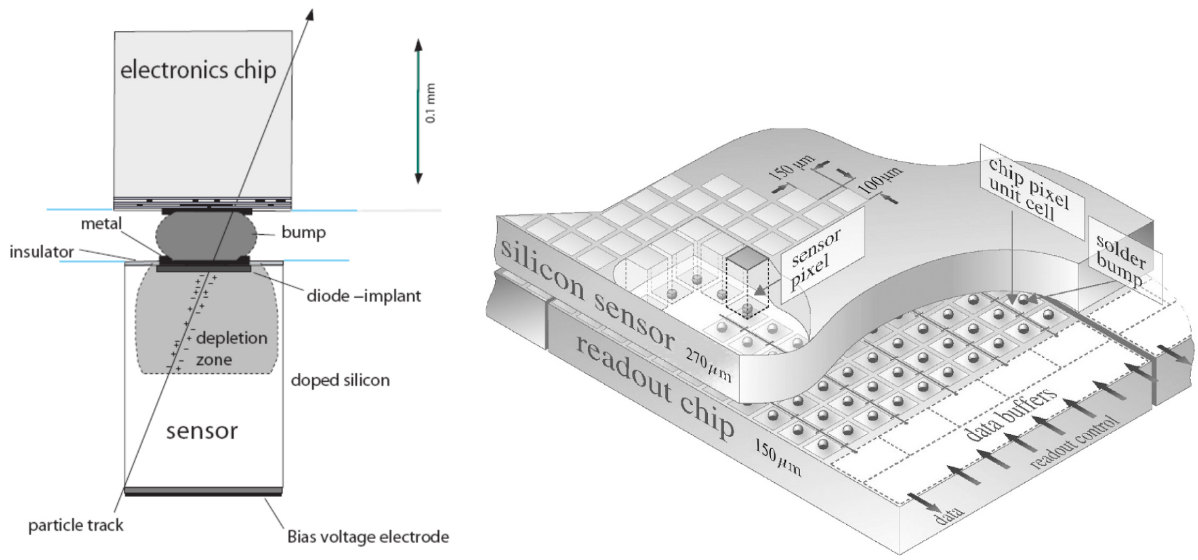

(a) (b)

Figure 5: a) Cross-sectional drawing of a pixel composed of silicon sensor and individual pixel unit cell on the readout chip connected via bump bonding.
b) Sensor and readout chip are segmented into an array of pixels which are read out individually. Ref: [1]

3 Calibration of Pixel Detector Modules

Because for the same amount of electron-hole pairs created in the silicon sensor, each pixel of the ROC would lead to a different output. Thus every 4160 circuits on the ROC have to be calibrated in order to know how many electrons are released in the silicon sensor. This can be achieved by a ROC-internal - well defined - calibration pulse, starting on the same place as the sensor electrons and running through the same circuit. The actual sensor pulse can then be expressed in those calibration-equivalent units, called "VCal"-units. The comparison between the deposited energy in the sensor and the VCal unit is achieved by the X-ray calibration.

This section also gives a kind of motivation to built the module holding setup. Furthermore it gives a little insight about the test routine and its limits.

3.1 Electric Pre-Calibration

Before the X-ray calibration could be carried out, some internal chip calibrations were required. These calibrations include basic functionality test and finding the right settings for the ROC and every PUC. These tests have to be performed every time a new chip were used or when experimental conditions (e.g. temperature) have changed significantly. All tests were implemented in the *psi46expert* software package run on a linux computer.
The first tests were called *PreTest*, *FullTest* and *Trimming*. These tests contained for example [1]

- Loading of several parameters from configuration files.
- Test if ROC DACs are programmable.
- Calibration of the address level decoder.
- Pixel alive test
- Trim bit test
- Address level decoding
- Threshold is set globally with the *VthrComp* DAC
- Using the four trim bits in each PUC to obtain a narrow threshold dispersion of all pixels

just to mention some of them.

3.1.1 Pulse Height Calibration

The Pulse Height Calibration or PHCal is also a ROC-internal calibration, carried out by the *PHCalibration*-routine in the *psi46expert* software. "The amount of charge being read out from the chip is referred to as detector signal or pulse height measured in ADC counts [...]. The behavior of this pulse height as a function of initial charge, whether generated in the sensor or injected as calibration pulse, is of major interest for the calibration measurements". [1]

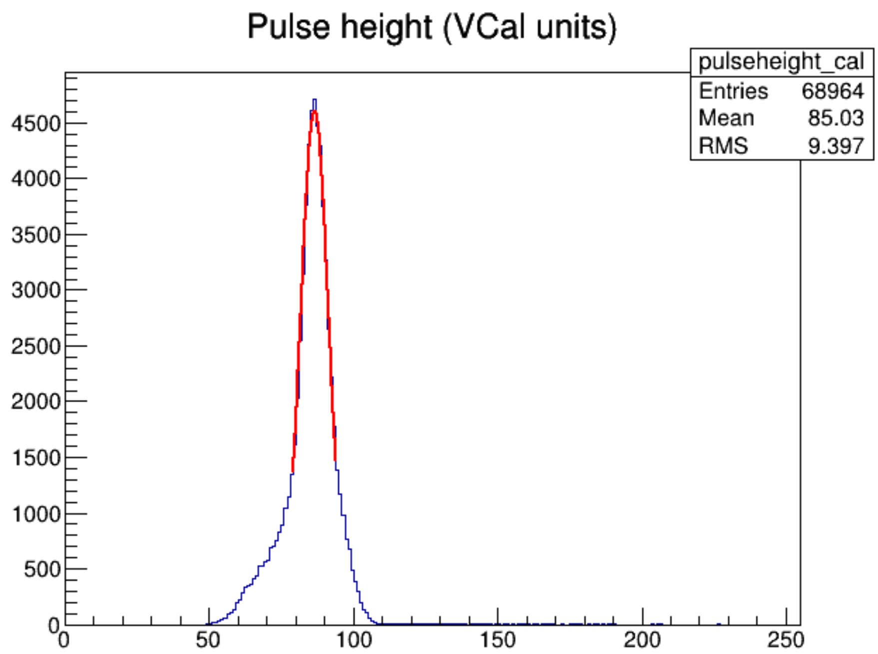

Figure 6: The histogram of the *PHCalibration* was fitted by a gaussian curve to determine which VCal value is most possible. The horizontally axis are the corresponding VCal units and the vertically axis the counts.

3.2 X-ray energy calibration

The goal of the X-ray energy calibration is to find the linear relation between the measured *Vcal* and the energy deposited in the sensor. With the knowledge of the deposited energy the penetration point of a particle track can be determined more precisely since the particle track excites also adjacent pixels. The penetration point can then be calculated by evaluating the center of gravity of this charge distribution.

Calibration means a comparison between two quantities, one with known magnitude or correctness. The X-ray energy calibration is achieved by a known photon energy. The X-ray tube (Fig. 7 a) irradiates a target material (Fig. 7 b) which atoms gets excited and emits primary photons with the well known K_α transition energy.

The deposited energy in the sensor by K_α photons can be translated in electron-hole pairs generated in the silicon sensor by

$$N_{e^-} = \frac{E_{K_\alpha}}{3.6\text{eV}} \tag{1}$$

since the excitation of one electon-hole pair in silicon needs 3.6 eV. With the measured *Vcal* in DAC units, we get a direct relation between *Vcal* and the number of excited electrons in the sensor which equates a data point in the electrons-*Vcal* diagram as shown in figure 9.

3.2.1 K_α energy

In table 1 the K_α transition energies are listed. Furthermore from these energies the equivalent number of excited electrons in the sensor according to equation 1 are given.

Material	K_α [keV]	N_{e^-}
Mo	17.49372	4833
Ag	22.162917	6122
Sn	25.27136	6981
Ba	32.193262	8893

Table 1: The K_α-energies of the different targets. With an energy gap of 3.62 eV of Si, the number of excited electrons N_{e^-} are calculated using equation 1.

3.2.2 Measurement setup

All measurements were taken in the lab of Prof. Wallny at the institute of particle physics (IPP) at ETH Zurich. The X-ray energy calibrations were accomplished in a *Seifert Analytical X-ray*-box shown in figure 7. This box contained three main parts:

a) The X-ray tube with two shutters: One horizontally to expose the target magazine and one vertically to direct irradiate the setup.

b) A automatic movable target magazine in order to obtain second order radiation by well known K_α energy levels.

c) A box which contained the sensor. This box contained sensor cooling elements and a dry air atmosphere in order to avoid condensation. A closer look at the sensor box is shown in figure 8.

3.2.3 Measurement Results

The analyzed chip was an analoge dose 0 chip. After the pretests have been carried out, the X-ray calibration was taken with the four different targets molybdenum, silver, tin, and barium. In order to analyze the temperature dependence of the X-ray calibration, the whole procedure was carried out for six different sensor temperatures reaching from -30°C to 20°C.
All measured data are shown in the appendix A in figure 20.

3.3 Leakage current $I_{\mathbf{leak}}$ test

During the running time of the LHC, the sensors of the CMS Pixel Detector are exposed to a huge amount of radiation. This radiation damages the sensors significantly. Thus, in this section we want to set the focus on the leakage current of irradiated and unirradiated sensors. The irradiated chips were irradiated by a high energy proton beam, which simulates a complete lifetime of constant measurement radiation.
In order to perform some tests with irradiated sensors we have to make sure that the leakage current is not too high. Otherwise the bias voltage of the sensor drops in order not to damage the chip. As one can easily see in figure 10 one has to cool down an irradiated chip to at least 0°C.

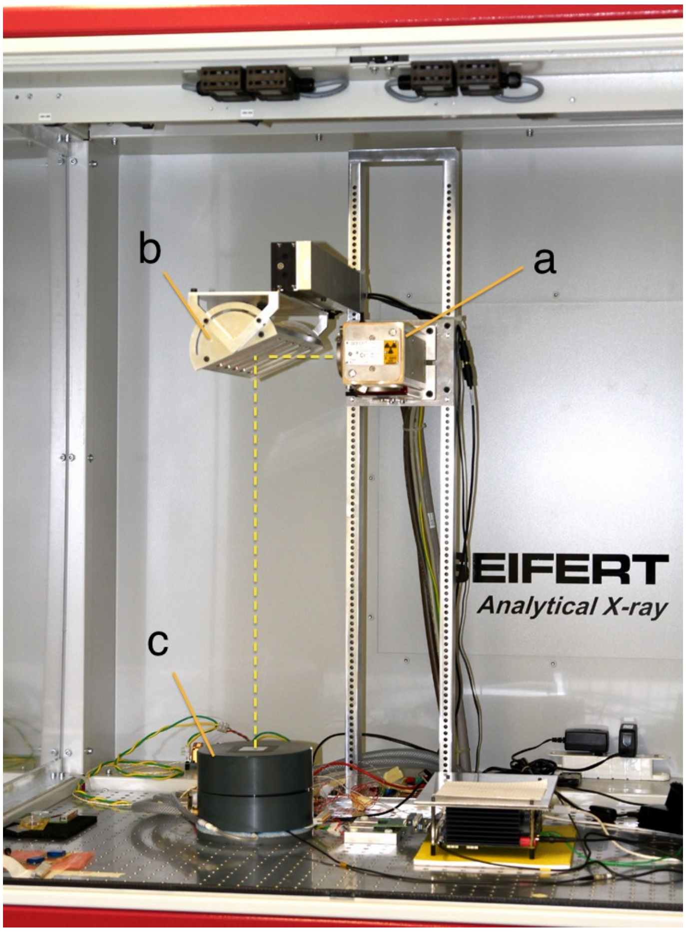

Figure 7: The used X-ray box to achieve X-ray energy calibration. a) X-ray tube b) movable target magazine c) sensor box (only singlechip sensors)

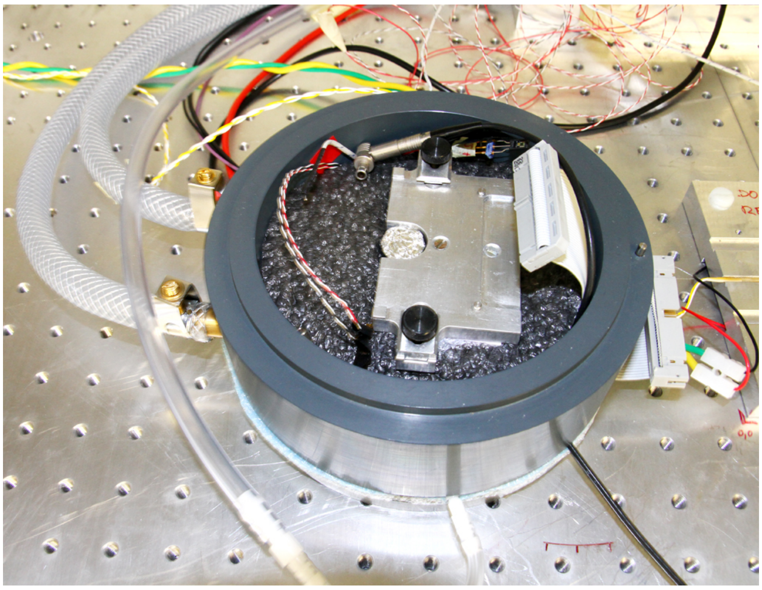

Figure 8: Single chip holding setup to achieve the X-ray energy calibration at steady temperature. It contains water cooled peltier elements, dry air atmosphere to avoid condensation, temperature and humidity sensors and several sensor connections.

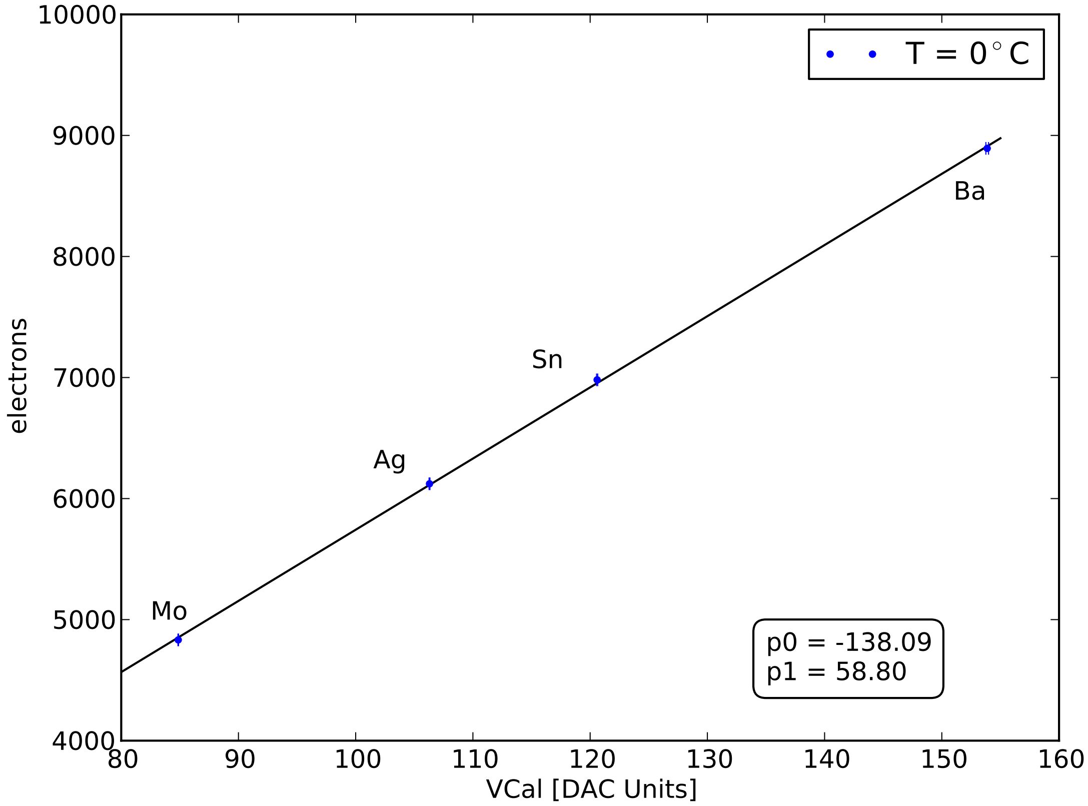

Figure 9: Example of a X-ray calibration. The number of electrons released are plotted as a function of the measured Vcal units. These four measurements were taken at 0°C.

3.4 Analysis

In this section we want to set our focus on the measurement results of this section in order to give a motivation why the module holding setup is necessary and what main goals it has to fulfill.

Let's start with the X-ray energy calibration which results are collected in appendix A figure 20. The slopes of these linear fits were determined and are shown in figure 11. In order to test if the slopes were temperature dependent, we fitted the resulting curve in figure 11 with a constant function and determined its χ^2/ndf-value. With a value of about 11.4 this is a bad fit and thus we suppose a temperature dependency.

If we took a closer look on the linear fits in figure 11 we observed that the *Ba*-datapoint of all measurements are not as good aligned as the other three data points. As a matter of fact it reduces the slope significantly especially for lower temperatures. Since the correct fit function should be a hyperbolic tangent, this datapoint falsifies the linear area a little bit. Due to that fact we calculated the linear fits again by ignoring the *Ba* datapoint. The resulting linear fits are shown in appendix A figure 21 and from that the new slopes are shown in figure 12. By fitting the newer slope curve with a constant function, we got a χ^2/ndf-value of about 1920 which indicates a temperature dependency for sure.

In order to determine the deposited energy precisely, we have to consider the temperature dependence of the chip-calibration and thus we need calibrations of different temperatures.

Furthermore as explained in section 3.3 and shown in figure 10, irradiated sensors have a high

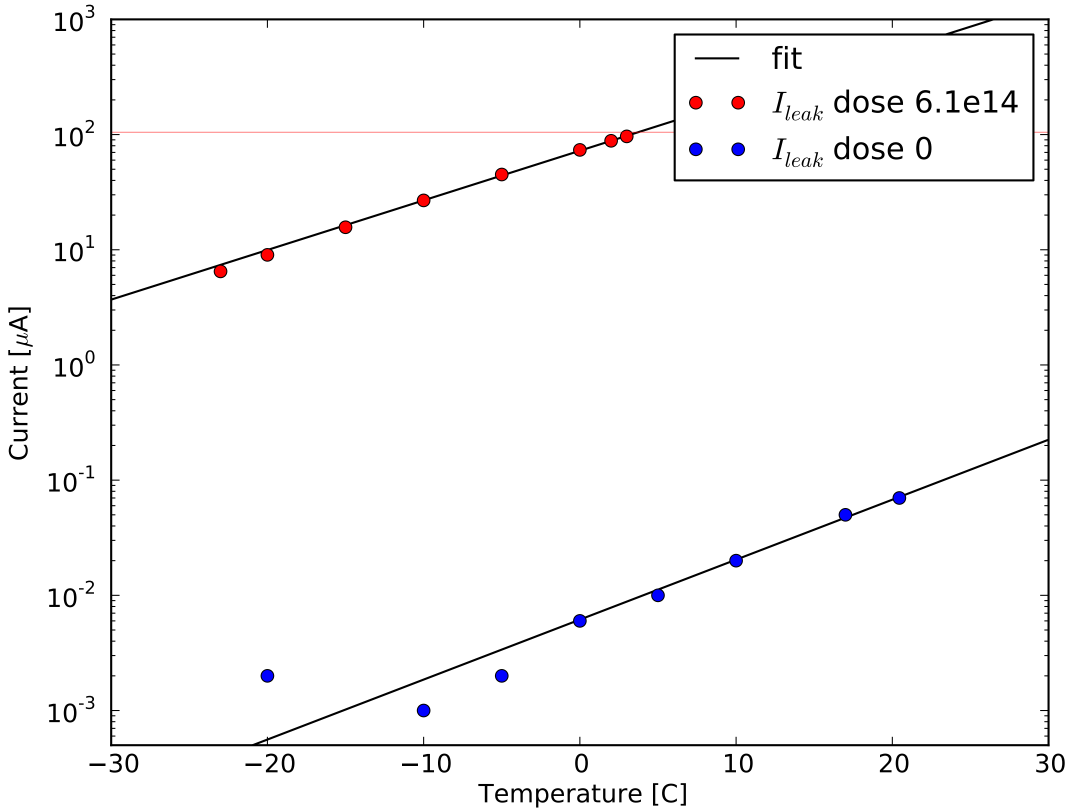

Figure 10: Plot of the leakage current I_{leak} as a function of the temperature of an irradiated and an unirradiated sensor. The horizontally red line marks the set upper limit of the leakage current in order not to damage the sensor. Higher leakage current would cause a drop of the bias voltage on the sensor.

leakage current and hence have to get cooled down below 0°C in order to take any measurements. This can only be achieved in a low-humidity environment.
As a conclusion we need a setup to perform X-ray measurements on pixel modules at low temperatures (about -20°C). This can be achieved by the new module holding setup.

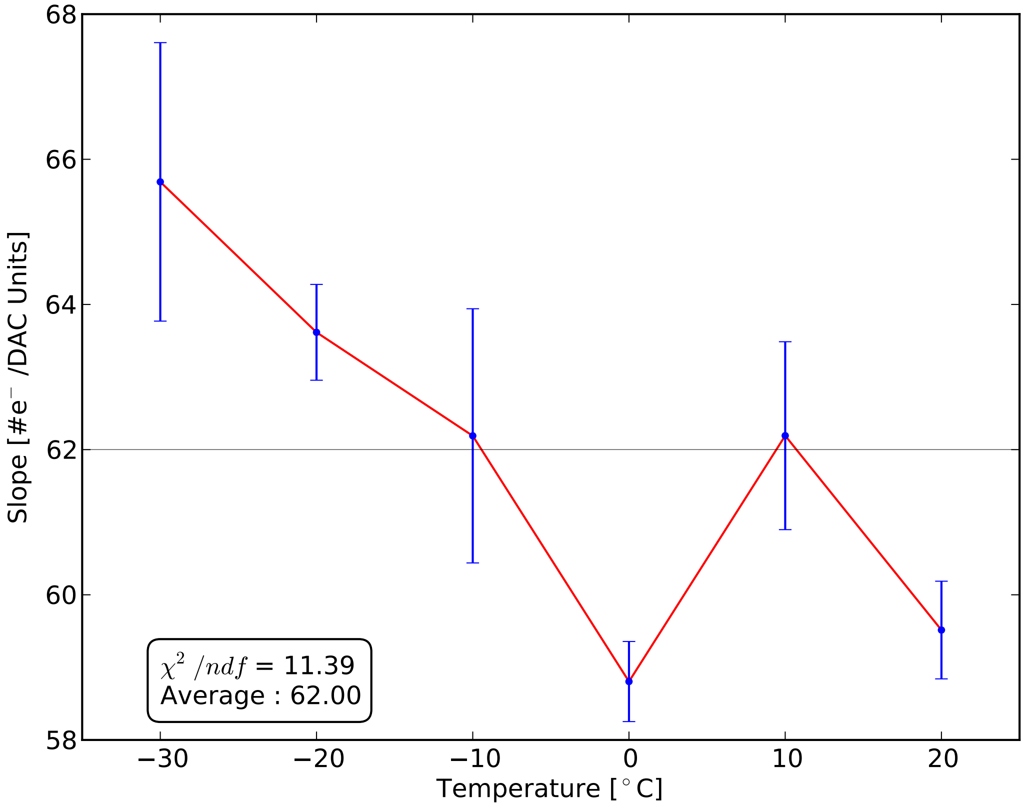

Figure 11: The slopes evaluated by the linear fit functions as shown in appendix A figure 20 as a function of the sensor temperature. For a constant fit function as shown as a horizontal line we get a χ^2 of about 11.4 which indicates this as a bad fit. Hence we suggest that the slope of the calibration (and thus the calibration itself) is temperature-dependent.

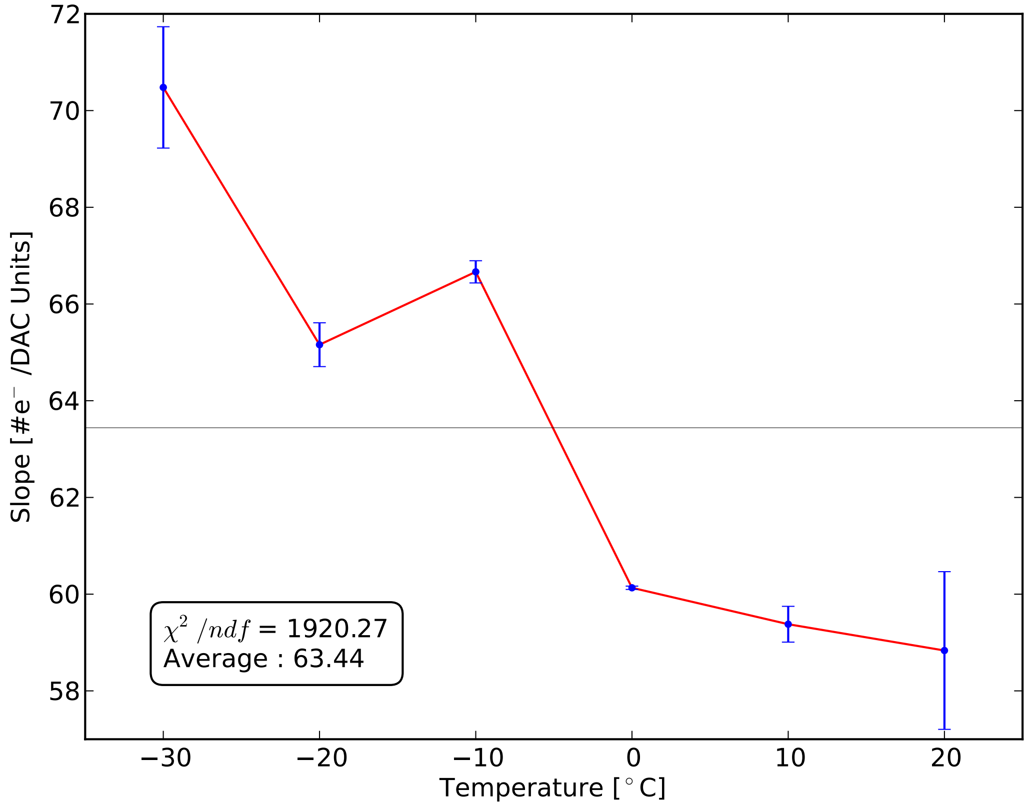

Figure 12: The slopes evaluated by the linear fit functions as shown in appendix A figure 21 as a function of the sensor temperature. For this plot, the data points of barium have been ignored. For a constant fit function as shown as horizontal line we get a χ^2 of about 1920 which indicates this as a really bad fit. Hence with this set of data points we would say that the slope of the calibration (and thus the calibration itself) is temperature-dependent for sure.

4 Moduleholder Setup

The module holding setup has had to fulfill the following points:

- X-ray energy measurements of four CMS pixel modules on aluminum handles
- full temperature range from -30°C to +30°C for stage II
  - adjustable and steady temperature (stage I / stage II)
  - uniform temperature distribution (stage I / stage II)
- to achieve an uniform temperature distribution, the peltier elements have also to get cooled uniformly
- vacuum to suck down the modules for a better thermal connection
- ensure no damaging of the modules during mounting and dismounting process
- no distorted results from second order radiation from nearby metal parts such as metal screws
- possibility of measuring single chips
- dry air atmosphere for stage II
- cable management out of the setup without violate above points
- esthetic appeal

4.1 Stage I Parts

4.1.1 Groundplate

The Groundplate serves as a basis for the whole setup. On this aluminum plate not just the main parts are fixed but also the electronics and connections for dry air and vacuum can be fixed. Furthermore it simplifies the installation and dismounting of the setup in the X-ray box.

4.1.2 Cooling element

The major task of the cooling element is to dissipate the heat from the peltier cooler. In doing so, it is important to cool the 6 peltier elements uniformly. In order to keep this uniform cooling, we considered a design shown in figure 13.

The water flow Figure 19 shows a transparent view through the cooling element. In order to prevent a temperature gradient, we designed it in a way so that the water between two channels flows in opposite directions.

4.1.3 Backup unit

The Backup unit consists of two connected parts. One of them is made of Polyoxymethylene (POM) and serves as a thermal insulation. The entire Backup unit supports the upper plate in order to avoid bending. Without the Backup there is a much higher risk of damaging the sensitive peltier cooler elements.

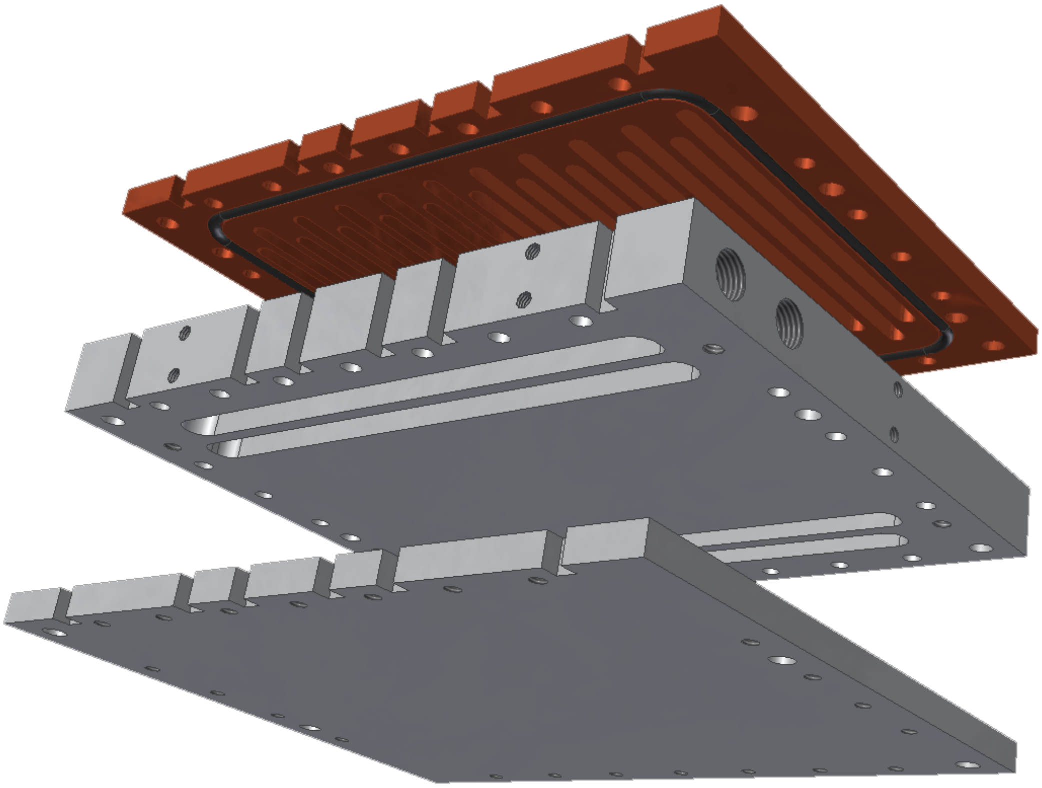

Figure 13: The Cooling element consists of three parts: Lowerplate, Coldplate and Copperplate

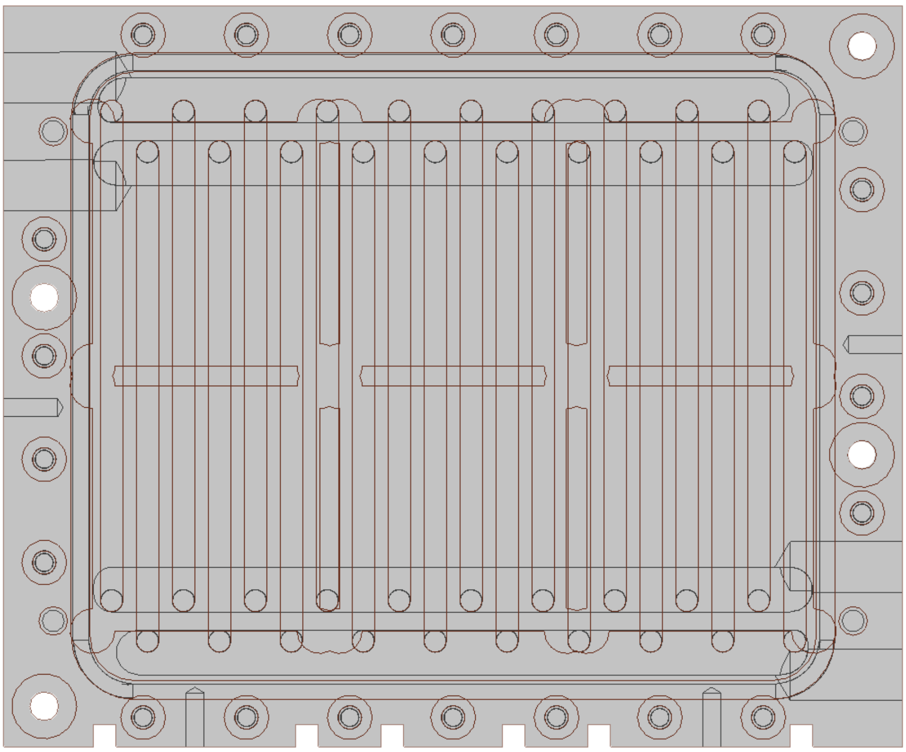

Figure 14: A transparent view through the cooling element. One can easily see the 4 water connections on the top left and on the bottom right corners.

4.1.4 Upper plate

The upper plate as shown in figure 15 is the most complicated part. It is designed to get cooled down in order to apply low temperature measurements. To monitoring the cooling status there

can be three temperature sensors and two humidity sensors fixed on the surface. Furthermore a complicated distribution system has been designed to bring the dry air next to the modules.
There is a possibility to use a vacuum pump to suck the modules down in order to achieve a good thermal connection between the modules and the module holder.

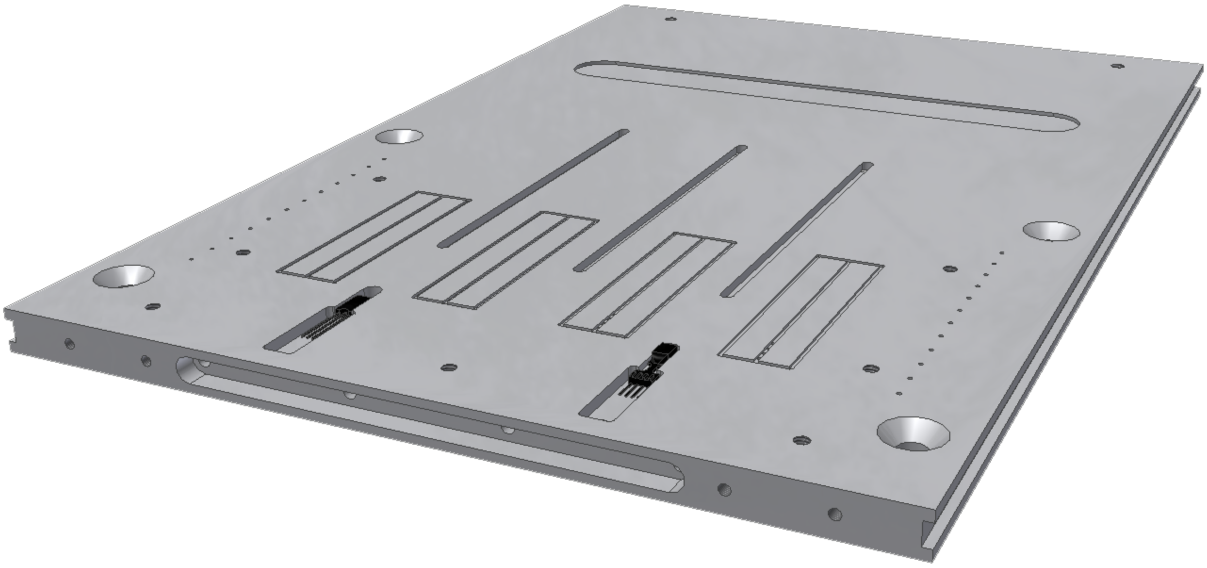

Figure 15: The upper plate has several features; different temperature and humidity sensors, distribution system to cool down the dry air and bring it to the modules, vacuum etc.

4.1.5 Module fixing parts

In order to fix the modules on the upper plate and achieve a good thermal connection, we designed the fixing unit in a way that makes it also easy to fix 4 modules at the same time. The modules get pushed against the Moduleclip by four individual fastener. These parts can be seen in figure 16.

4.2 Stage II Parts

In order to prevent condensation at lower temperatures, every part from stage I except for the groundplate has to get enclosed in a casing which is flooded by dry air. For this casing are some more parts required. These are the stage II parts.
In stage II the upper plate is surrounded by a sponge rubber to avoid thermal connection between the upper plate and the walls of the casing. It also serves as a seal of the dry air guidance.
The design of stage II is shown in figure 17.

4.2.1 Distance pieces

The distance peaces provide the correct distance to the stage I parts, and thus also a correct compression of the sponge rubber, avoiding thermal connection.

4.2.2 Walls

The aluminum walls contain all necessary holes to feed all cables and water connectors trough it. The design of the casing allows the use of thin metal sheets, preventing a heavy setup.

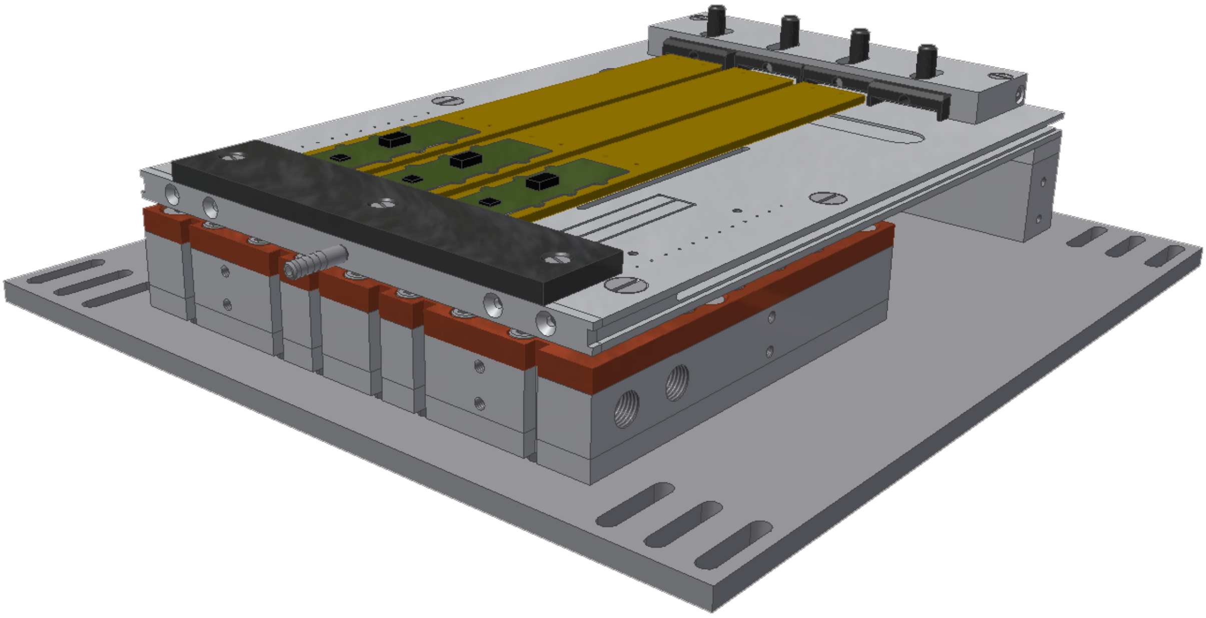

Figure 16: Stage I: The upper plate has several features; different temperature and humidity sensors, distribution system to cool down the dry air and bring it to the modules, vacuum etc.

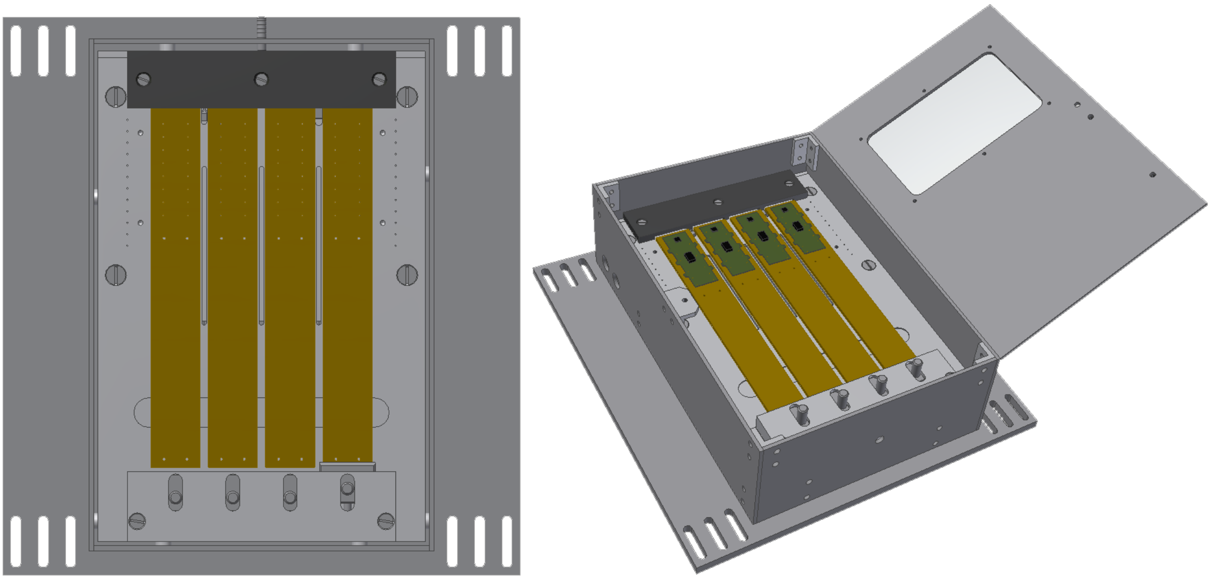

Figure 17: Stage II: On the left picture one can see the gap between the walls and the upper plate, determined by the distance peaces. In between there would be the sponge rubber (not drawn). The right picture shows the stage II with mounted cover plate, including the window.

4.2.3 Insulation and cover plate

The insulation elements are mounted on the inner side of the walls and inside the top cover plate. The cover plate has a window in it, consisting of thin acrylic glass. It is connected to a wall by a hinge-joint and has a hand gear outside in order to open the case.

4.3 Cooling element pressure test

The water channels in the cooling element as one can see in figure 19 feed an area of about 0.022m^2. The cooling element was construed for water pressures up to 3 bar hence for a pressure induced force of about 660 N. However in the lab, we have a cooling water pressure of about 8 bar. Hence it was necessary to verify that the cooling element resists higher pressure in the first place and second that it does not bend too much. The test showed that the cooling element is leakproof also for higher pressures. With a static pressure of 8 bar, the middle of the surface bends about half a millimeter. That's not quite much, but when it is jammed with the peltier elements between the groundplate and the upper plate, the bending of the cooling element could damage the inelastic peltier elements.
In order to analyze the bending and the pressure in the dynamic case, we mounted a pressure control valve in front of the cooling element and measured the outflow for different pressures. Hence we are able to estimate the effective pressure in the dynamic case by measuring the waterflow. Unfortunately the used pressure control valve only works up to 4 bar. The waterflow as a function of the measured pressure is shown in figure 18 as red dots. The waterflow without the pressure control valve is plotted as a horizontal line. Even for the full pressure in the dynamic case, the cooling element does not bend significantly. Thus it is important to provide the outward flow in order not to damage the peltier elements due to the bending of the cooling element.

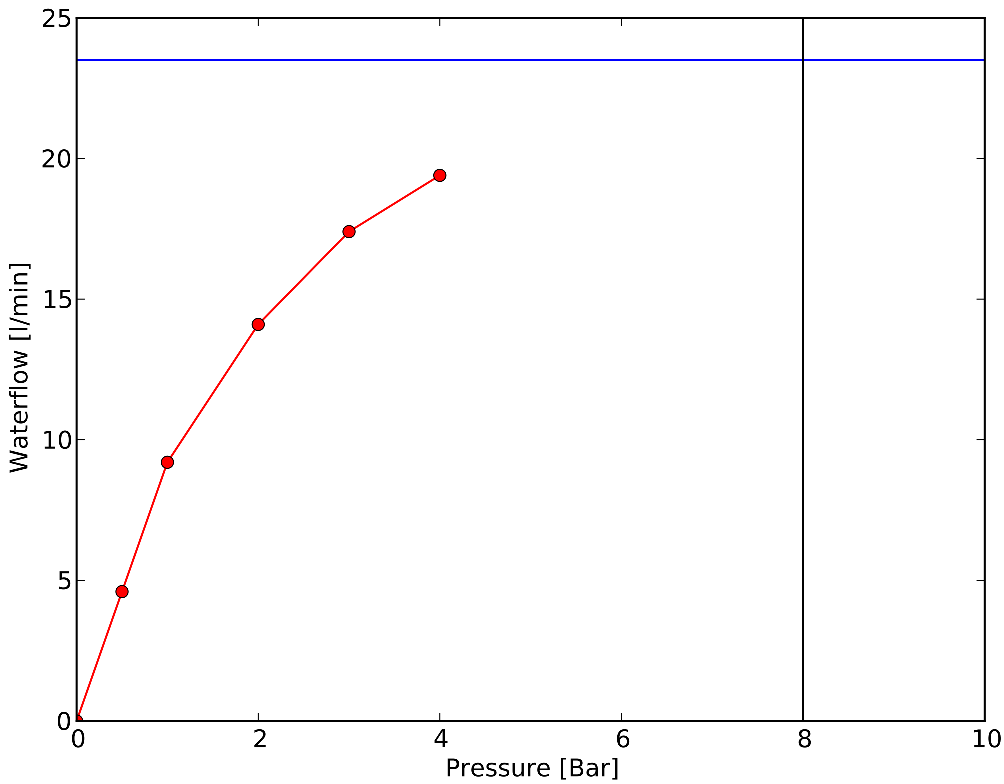

Figure 18: The waterflow trough the cooling element as a function of the input pressure. The horizontal line marks the waterflow when the cooling element was connected to the full pressure, which should be about 8 bar. During the dynamical pressure tests, the cooling element did not bend significantly.

5 Further Steps

In order to finish stage II, the following main tasks have to be performed:

- find a suitable handle as a standard part for the top cover plate
- find a suitable hinge-joint for the top cover plate
- internal connections for the modules
- internal dry air connection on the M10 screw thread in the backup unit.
- peliter element power supply, sensor cables and dry air connections in the side wall
- create the engineering drawings for the additional parts

If these tasks are fulfilled, stage II can be manufactured and assembled.

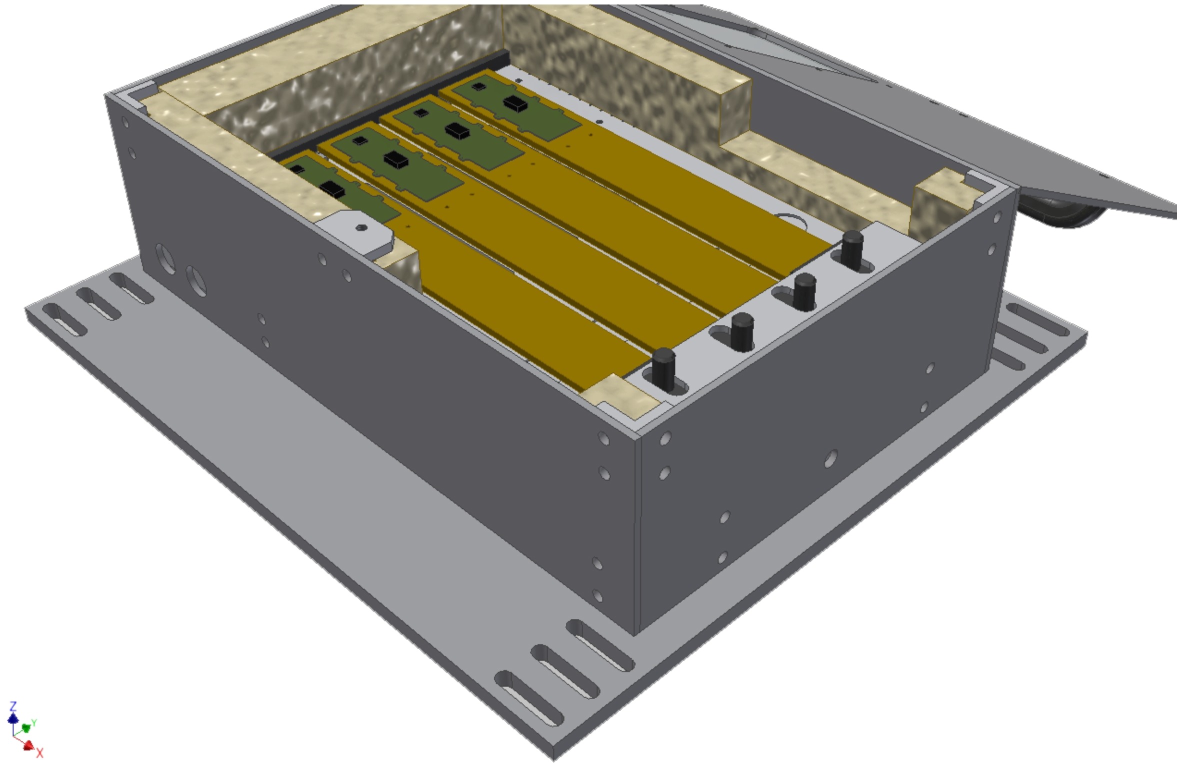

Figure 19: Stage II of the module holding setup

6 Conclusion

Although the semester project was quite time-consuming, it was also a very interesting diversion to the daily routine of the studies. Also the collaboration with Marco Rossini and Jan Hoss was very informative. We had a huge benefit of each other, because I brought the experience how to technical draw parts that are manufacturable and on the other hand, they gave important advices from the physical point of view of the measuring process with the X-ray tube. Thus together we found a design that is both manufacturable and fulfills all important tasks.

Working in the lab and performing X-ray measurements was also very interesting and instructive. Therefore after finishing my physics studies I absolutely can imagine to work in the field of experimental physics - especially in the field of particle physics.

Appendices

A X-Ray calibration plots

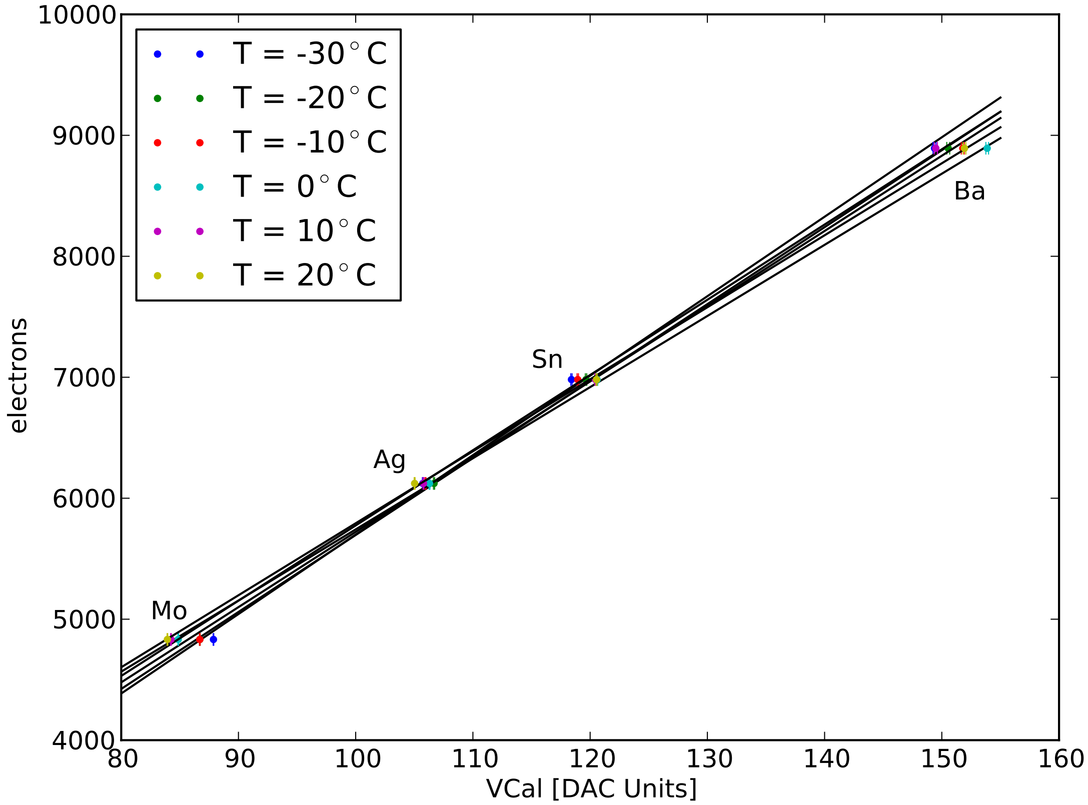

Figure 20: Collection of all measured data with its linear fits.

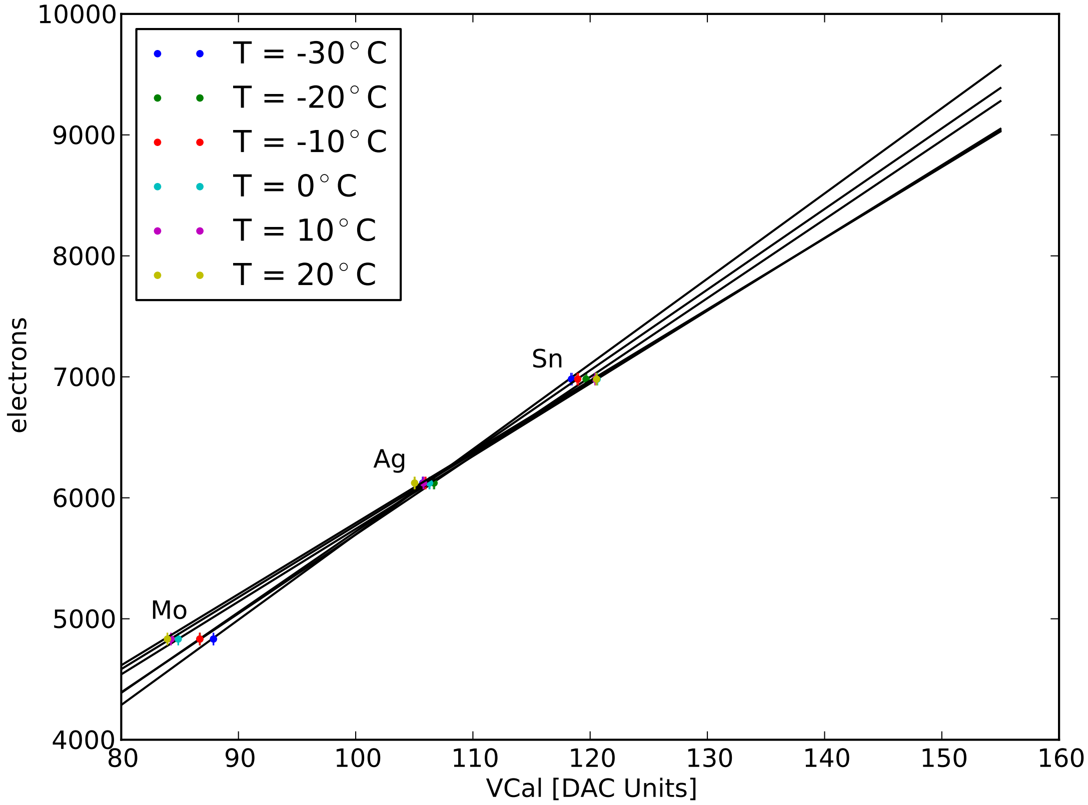

Figure 21: Collection of all measured data with its linear fits, but with the Ba-datapoint ignored.

B List of Parts for stage I

Pos.	Name	Quantity	Material
1	Groundplate	1	Aluminium
2	Lower Plate	1	Aluminium
3	Coldplate	1	Aluminium
4	Copperplate	1	Copper
5	Backup	1	Aluminium
6	Backup insulator	1	POM
7	Upper plate	1	Aluminium
8	Vacuum closure	1	Aluminium
9	Vacuum connection	1	Steel
10	Moduleclip	1	POM
11	Fastener	4	POM
12	Fastener guidance base	1	Aluminium
13	Fastener guidance top	1	Aluminium

Table 2: Selfemade Parts

Pos.	Name	Quantity	Manufactor	Dimensions	Catalog Nr.
101	O-Ring	2		185x3	
102	Pressure spring	4	www.durovis.ch	D8 $L_0$24.5 L_n5.91	42/5/2
103	Pressure spring	4	www.durovis.ch	D6.3 $L_0$20 L_n4.68	40/5/2
104	Pressure spring	4	www.durovis.ch	D6.3 $L_0$17 L_n5.6	52/4/2
105	Peltier element	6		50x50x4.3	
106	Water connector	4			
107	Power supply	1			

Table 3: Standard parts and parts of other manufacturers

C Engineering drawings for stage I

C.1 Groundplate

C.2 Lower Plate

C.3 Coldplate

C.4 Copperplate

C.5 Backup

C.6 Backup insulator

C.7 Upper plate

C.8 Vacuum closure

C.9 Vacuum conection

C.10 Moduleclip

C.11 Fastener

C.12 Fastener guidance base

C.13 fastener guidance top

References

[1] *X-Ray Calibration of Pixel Detector Modules for the Phase I Upgrade of the CMS Experiment,* Diplomarbeit Jan Hoss, Karlsruhe, 27. September 2012

[2] CERN, *The LHCb Detector* [Online], 2013-08-20, http://lhcb-public.web.cern.ch/lhcb-public/en/detector/Detector-en.html

[3] CERN, *CMS detector design* [Online], 2013-08-20, http://cms.web.cern.ch/news/what-cms

[4] CERN, *CMS Tracker detector* [Online], 2013-08-20, http://cms.web.cern.ch/news/silicon-pixels